# ELECTRIC FIELD DEPENDENCE OF PHOTOEMISSION FROM N- AND P-TYPE SI CRYSTALS

S. Mingels*, B. Bornmann, D. Lützenkirchen-Hecht, G. Müller
University of Wuppertal, Faculty C – Physics, Gaußstr. 20, 42119 Wuppertal, Germany
C. Langer, C. Prommesberger, R. Schreiner
Regensburg University of Applied Sciences, Faculty of Microsystems Technology, Seybothstr. 2, 93053 Regensburg, Germany

*Abstract*

The performance of free electron lasers depends on the brilliance of the electron source. Nowadays photocathodes (e.g. $Cs_2Te$) are used despite of their high emittance. To develop robust and more brilliant cathodes we have built up an UHV system which enables systematic photoemission (PE) measurements with a tunable pulsed laser (hν) at high electric fields (E). First results on Au and Ag crystals revealed only low quantum efficiency (QE) due to fast electron relaxation. Hence, we have started QE(hν,E) investigations on n- and p-Si wafers. Resonant PE was observed above as well as below the work function Φ, which can be assigned to optical transitions in the electronic band structure or explained by thermally excited states at the bottom of the conduction band. As expected, only low QE values were achieved even for n-Si probably due to surface oxide. Moreover, a significant rise of the QE peaks above Φ were obtained for n-Si at E > 8 MV/m but limited by the occurrence of parasitic field emission from dust particles.

## INTRODUCTION

High brightness electron sources are crucial for large FELs [1] like LCLS or XFEL with intense beams or novel compact x-ray lasers where coherent synchrotron radiation is generated by means of the ion cores in a single crystal [2]. State of the art $Cs_2Te$ photoemission (PE) cathodes provide high peak currents up to 50 A in short (~20 ps) pulses [3]. However, their brightness is limited by the thermal emittance, which results from the kinetic surplus energy and transverse momentum. Recently, a geometric mean emittance of 0.70 mm mrad for a bunch charge of 1 nC was achieved with $Cs_2Te$ at PITZ [4]. Moreover, alkali-based photocathodes require extreme vacuum < $10^{-8}$ Pa for sufficient lifetime of high quantum efficiency (QE).

An attractive alternative to generate highly brilliant electron beams from more robust cathodes is photo-induced field emission (PFE) which might combine fast switching of PE with the low emittance of field emission (FE) [5]. In order to find a suitable PFE material, we have recently set up an UHV apparatus with electron spectrometer in adjustable triode configuration which is designed for high electric field E as well as tunable laser illumination of the cathode [6]. First PFE measurements were performed on Si tip arrays in dc mode, i.e. with an old Auger electron spectrometer and a green laser. As next step, a ns-pulsed laser tunable over a wide range (0.54 – 5.90 eV) was installed, which enables indirect but prevents direct spectroscopy of the PFE electrons. Au and Ag crystals yielded only moderate QE(5.8 eV,18 MV/m) = 9×10-5 [7] due to fast electron relaxation in the highly populated conduction band. Therefore, we have started to investigate the PFE of slightly doped semiconductors, e.g. flat n-Si(111) and p-Si(100) crystals.

## EXPERIMENTAL

The actual PFE measurement apparatus is shown in figure 1. The vacuum system consists of a load-lock and a main chamber with a base pressure of $10^{-5}$ Pa and $10^{-7}$ Pa, respectively. The load-lock contains a transport system for cathode and gates and a ion sputtering system for in-situ cleaning, and a gate valve enables quick sample exchange [6]. The main chamber contains a triode system, which consists of a cathode, a gate, and a spectrometer. Figure 2 shows the rotatable excentric cathode holder opposite to the electron extractor gate in detail. The cathode holder is mounted on a linear piezo drive by which the gap distance $d_{gap}$ can be set with µm resolution. The support rod can be retracted over 40 mm for cathode and gate exchange. The mesh gate is fixed to a truncated hollow cone support system (2.6 mm inner and 3.0 mm

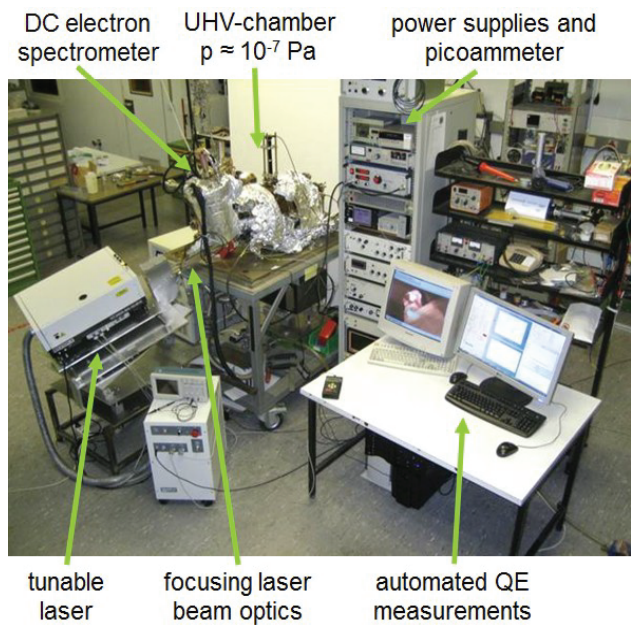


Figure 1: Photo of the PFE measurement apparatus.

*s.mingels@uni-wuppertal.de

ISBN 978-3-95450-126-7

outer diameter) which can be tilted by screws and controlled by a long range microscope with a precision of 10 µm. Applying a gate voltage up to 20 kV at a gap down to 50 µm gives a maximum electric field E of 400 MV/m at the flat cathode surface. For the actual mesh gate the field homogeneity is better than 95%. The cathode current is measured with a picoammeter (Keithley 6485A), while the gate current can be estimated by means of the HV power supply. Most of the transmitted electrons reach the grounded spectrometer nozzle, which is located on axis about 40 mm behind the gap.

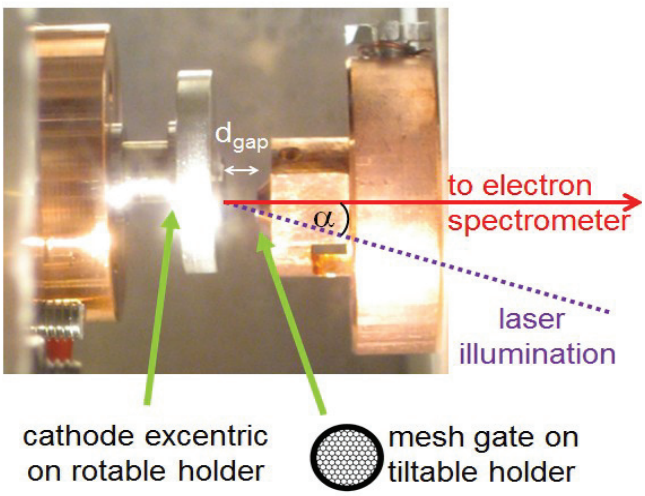


Figure 2: Photo of the cathode-gate configuration. The Cu mesh has a hexagonal geometry, a lattice constant of 254 $\mu$m, a thickness of 18$\mu$m, and a transparency of 85%.

The cathode illumination is performed through a quartz window and the gate by means of a pulsed (3.5 ns, 10 Hz repetition rate) tunable OPO Laser (Ekspla NT342A-SH). Its gap-free energy range (hν = 0.54 – 5.90 eV, λ = 2300 – 210 nm) is divided into three outputs, i.e. for IR (0.54 – 1.75 eV), visible (1.75 – 2.95 eV) and UV light (2.95 – 5.95 eV). The light is vertically (IR and UV) or horizontally polarized (visible) with a spot size of ≈ 4 mm (Gaußian profile), a divergence of < 2 mrad, and a spectral linewidth of < 5 $cm^{-1}$. It hits the cathode surface under an angle α (16° horizontally, 17° vertically) and can be focused by an plano-convex quartz lens, which is automatically adjusted depending on hν. The output energy of the OPO laser $W_{OPO}$ depends linearly on that of the driving Nd:YAG laser ($W_{pump}$ < 75 mJ at 355 nm) with a range-dependent offset. It was measured in the UV range with a pyroelectric sensor as shown in figure 3.

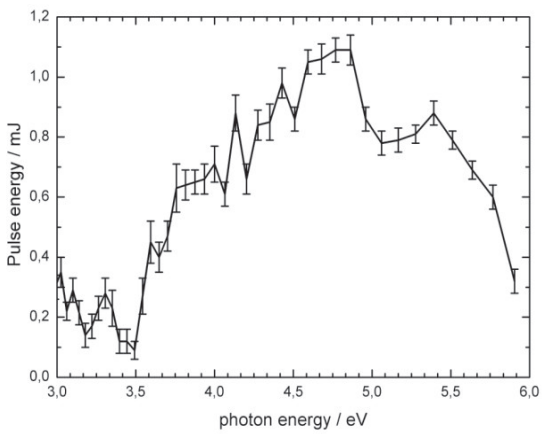


Figure 3: $W_{OPO}$ for $W_{pump}$ = 62 mJ. The error bars result from the pulse-to-pulse fluctuations of $W_{pump}$ averaged by the pyroelectric sensor.

For the QE(hν,E) measurements the laser and the picoammeter are synchronized by a trigger which is given by the computer control system. The data acquisition and analysis is performed online by means of C# software. For the determination of QE, i.e. the ratio of emitted electrons and incident photons, the cathode current, $W_{OPO}$, the transparency of lens, quartz window and mesh gate are taken into account.

The Si crystal samples were obtained from commercial 2" diameter wafers cut into pieces. The n-Si(111) sample (1/6 of a floating-zone grown 280 µm thick wafer) is slightly P-doped (electric resistivity ρ ≈ 150 – 250 Ω cm). The p-Si(100) sample (1/4 of a Czochralski grown 254 µm thick wafer) is B-doped (ρ ≈ 13 – 30 Ω cm). The crystals were cut and fixed with silver epoxy on Al holders under cleanroom conditions (see figure 4). Nevertheless the samples were slightly dust-contaminated during their insertion into the load-lock. All Si samples are covered with a natural 10 nm thick oxide, which was not removed by ion sputtering yet to avoid additional surface roughness.

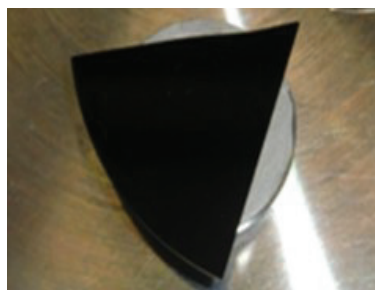

Figure 4: Photo of the n-Si(111) wafer on sample holder.

## RESULTS AND DISCUSSION

The QE(hν,E) measurements on the n-Si(111) and p-Si(100) samples were carried out with the settings listed in table 1, where ΔE and Δhν are the step widths. $W_{OPO}$ was measured at a fixed hν for the actual $W_{pump}$ and scaled according to figure 3. The symbols $d_{focus}$ and $J_{OPO}$ give the diameter of the laser spot on the cathode surface and the resulting energy density depending on hν.

The pure PE results for n-Si(111) and p-Si(100) were obtained at low E as shown figure 5. The slight differences of QE above 4 eV might be caused by the different crystal orientations. Surprisingly, the maximum values (0.13 and $0.10\times10^{-6}$) at 5.85 eV are lower than for Ag [7]. Possible reasons are natural surface oxides and intraband relaxation effects.



ISBN 978-3-95450-126-7

Table 1: QE(hν,E) Measurement Settings

| Parameter | n-Si(111) | p-Si(100) |
|---|---|---|
| $d_{gap}$ / µm | 500 | 450 |
| E / (MV/m) | 1.1 – 11.1 | 0.2 – 8.8 |
| ΔE / (MV/m) | 1.0 | 0.55 |
| hν / eV | 2.97 – 5.90 | 3.10 – 5.90 |
| Δhν / eV | 2 nm wavelength steps | |
| $W_{pump}$ / mJ | 30 | 27 |
| $W_{OPO}$ / mJ | 0.03 – 0.30 | 0.03 – 0.25 |
| $d_{focus}$ / cm | ≈ 0.1 | ≈ 0.1 |
| $J_{OPO}$ / (mJ/cm²) | 4 – 38 | 4 – 32 |

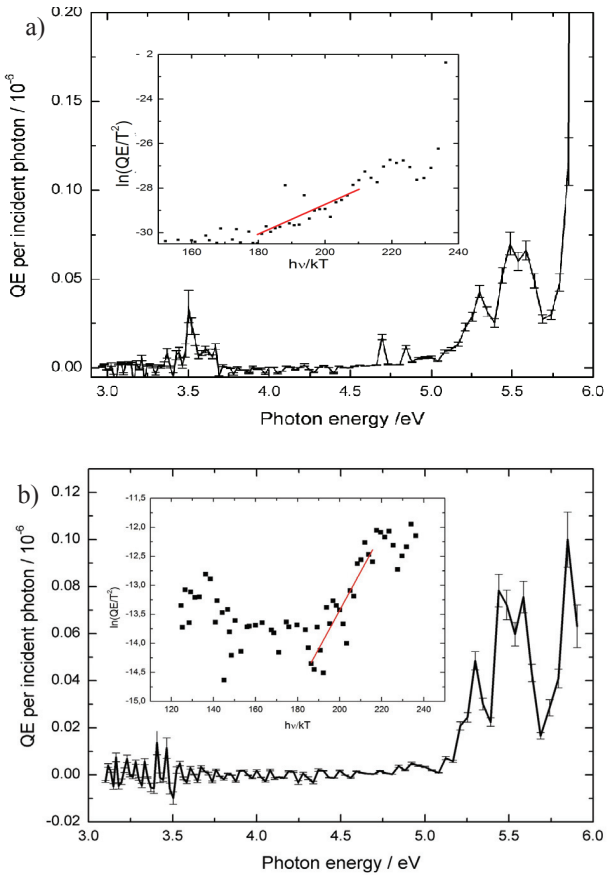


Figure 5: QE(hν) measured at T = 300 of a) n-Si(111) for 1.1 MV/m and b) p-Si(100) for 0.2 MV/m. The insets show the corr. Fowler plots with linear fit (red line).

The work function Φ can be determined by using Fowler's method [8,9]. For hν near the photoemission threshold it is predicted that

$$\ln\left(\frac{j_{PE}}{T^2}\right) = \kappa + \ln g\left(\frac{h\nu - \Phi}{k_B T}\right),$$

where $j_{PE}$ is the photoemission current density, κ is a constant, independent from T and ν, ln *g* is a function tabulated in [10], and $k_B$ is the Boltzmann constant. Band structure effects like resonant optical transitions are neglected in this formula, but usually Φ can be extracted as the x-intercept of a linear regression with a suitable offset. The fit results, Φ ≈ 4.4 eV for n-Si(111) and Φ ≈ 4.9 eV for p-Si(100) agree well with literature data ($\Phi_{Si(111)}$ = 4.6 eV and $\Phi_{Si(100)}$ = 4.91 eV, resp. [11,12]). The small difference of about 0.2 eV might be caused by the oxide layer or adsorbates.

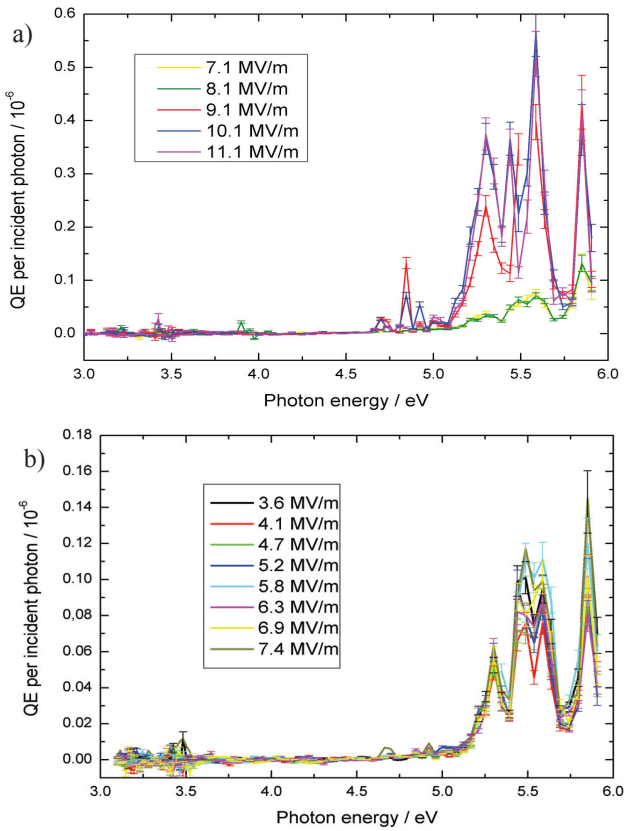


Figure 6: QE(hν) of a) n-Si(111) for E = 8.1 – 11.1 MV/m b) p-Si(100) for E = 3.6 – 7.4 MV/m.

The QE(hν,E) results are given in figure 6, where for clarity only curves for the high fields with significantly enhanced QE are displayed. Obviously, peaks occur at 5.3, 5.44, 5.59, and 5.85 eV independent of the doping, which clearly reflect band structure effects. The small features around 3.5 eV and 4.75 eV are more difficult to explain. Adding the bad gap of Si (1.14 eV) to the first value nearly reaches the measured Φ values. This suggests PE of thermally exited electrons from the bottom conduction band.

The field dependence of the QE peak is shown in figure 7. Clear effects start at 8 MV/m, but a field scaling law is not evident. Probably the QE increase is caused by E-induced Φ reduction (Schottky effect) due to local field enhancement.



ISBN 978-3-95450-126-7

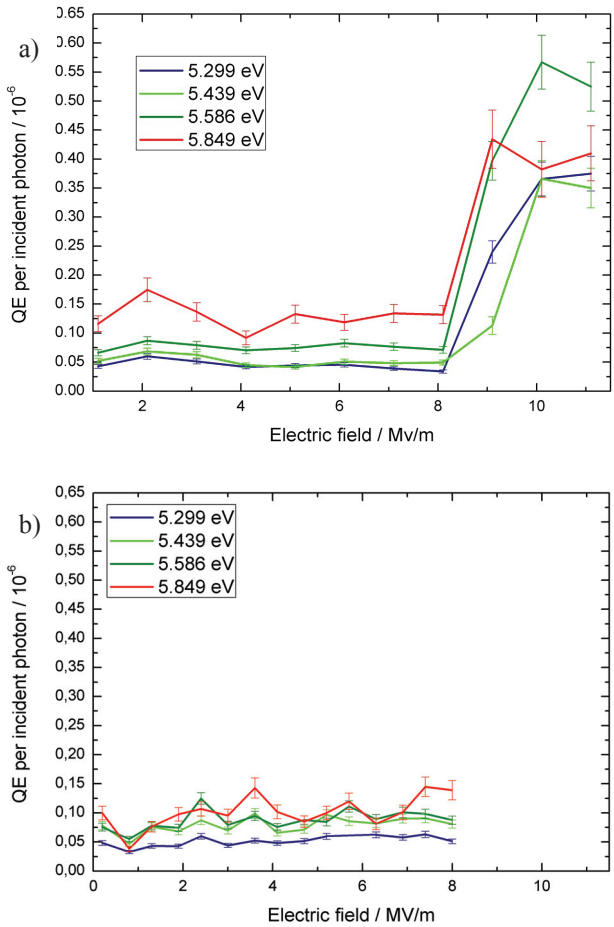


Figure 7: QE(E) of a) n-Si(111) and b) p-Si(100) for the main peaks in figures 5 and 6.

The peaks might be explained by transitions between points with high density of states in the band structure (e.g. at van Hove singularities). Beside direct (vertical) transitions also indirect ones can occur, if in addition the wave vector **k** is changed by means of scattering with phonons. The energy loss/gain for electron-phonon scattering is negligible. Possible transitions for the peaks are marked in figure 8 as blue (5.3 eV), green (5.44, 5.59 eV), and red (5.85 eV) arrows together with the yellow ones for the emission from the bottom of the conduction band. However, the final states lie just below $W_{vac}$, where Φ-lowering and broadening effect (e.g. thermal blurring) might enable the PE. Consequently, a further, Schottky-induced Φ-lowering probably explains the great increase of QE for E > 8 MV/m by shifting $W_{vac}$ well below the final states. It is unlikely caused by PFE, which should have a more exponential-like E-scaling. However, investigations at higher fields were hindered by parasitic FE from dust particulates yet.

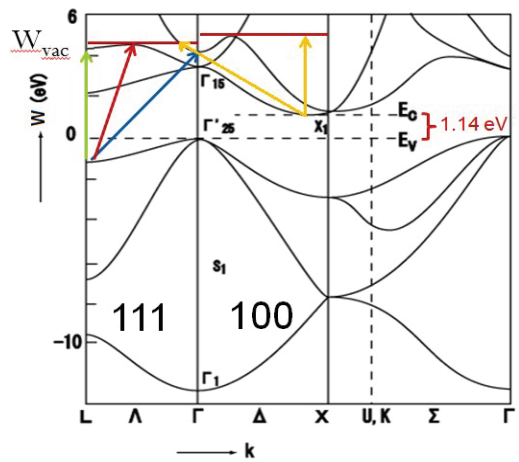


Figure 8: Electronic band structure of Si [13]. The colored arrows to the orientation dependent vacuum energy $W_{vac}$ suggest possible transitions for the peaks.

## CONCLUSIONS AND OUTLOOK

Systematic photoemission measurements of QE(hν,E) on n-Si(111) and p-Si(100) crystals resulted in reasonable work function values and revealed peaks as band structure effects. However, rather low QE ($< 0.2\times10^{-6}$) were obtained which might be improved by removal of surface oxides. Above $E \approx 8$ MV/m for n-Si(111) a strong QE increase by a factor of up to 8 was measured, but an early onset of enhanced FE prevented the observation of PFE.

Actually a $LN_2$ cooling and electrical heating of the cathode is installed, and a cleanroom environment at the load-lock is under construction. Furthermore, for in situ sample cleaning a ion source for soft sputter etching or a heating will be installed. Investigations on highly-doped wide-band-gap semiconductors (e.g. GaN) are planned. As soon as a promising PFE cathode is found, its emittance should be investigated at DESY Zeuthen or FZR Dresden.

## ACKNOWLEDGEMENT

This project is funded by the German Federal Ministry of Education and Research (BMBF) under project numbers 05K10PXA and 05K13PX2.

## REFERENCES

[1] D.H. Dowell, I. Bazarov, B. Dunhamb, K. Harkay, C. Hernandez-Garcia, R. Legg, H. Padmore, T. Rao, J. Smedley, W. Wan, Nucl. Instr. Meth. Phys. A 622, 685 (2010).

[2] C.A. Brau, B.K. Choi, J.D. Jarvis, J.W. Lewellen, P. Piot, Synchroton Radiat. News 25, 20, (2012).

[3] M. Altarelli, R. Brinkmann, M. Chergui, W. Decking, B. Dobson, S. Düsterer, G. Grübel, W. Graeff, H. Graafsma, J. Hajdu, J. Marangos, J. Pflüger, H. Redlin, D. Riley, I. Robinson, J. Rossbach, A. Schwarz, K. Tiedtke, T. Tschentscher, I. Vartaniants, H. Wabnitz, H. Weise, R. Wichmann, K. Witte, A. Wolf, M. Wulff, M. Yurkov, The European X-Ray Free-Electron Laser, Technical design report, DESY 2006-097 (2007).

[4] S. Rimjaen G. Asova, H.J. Grabosch, M. Groß, L. Hakobyan, I.V. Isaev, Y. Ivanisenko, M. Khojoyan, G. Klemz, W. Köhler, M. Krasilnikov, M. Mahgoub,



ISBN 978-3-95450-126-7

D.A. Malyutin, M. Nozdrin, A. Oppelt, M. Otevřel, B. Petrosyan, A. Shapovalov, F. Stephan, G. Vashchenko, S. Weidinger, R. Wenndorff, M. Hoffmann, H. Schlarb, D. Richter, I. Templin, I. Willi, Nucl. Instrum. Methods Phys. Res. A 671, 62 (2012).
[5] C.A. Brau, Nucl. Instrum. Methods Phys. Res. A 393, 426 (1997).
[6] B. Bornmann, S. Mingels, F. Dams, C. Prommesberger, R. Schreiner, D. Lützenkirchen-Hecht, G. Müller, Rev. Sci. Instrum. 83, 013302 (2012).
[7] S. Mingels, *Erweiterung der Apparatur und erste Ergebnisse zur photoinduzierten Feldemission*, Master's thesis, University of Wuppertal (2012), presented at FEL'12, Nara, Japan.
[8] R. H. Fowler, Phys. Rev. 38, 45 (1931).
[9] F. Wooten, R. N. Stuart, Phys. Rev. 186, 2 (1969).
[10] H. Simon, R. Suhrmann, *Der lichtelektrische Effekt*, Springer, Berlin-Göttingen-Heidelberg (1958).
[11] C. Sébenne et al., Phys. Rev. B 12, 3280 (1975).
[12] F .G. Allen, J. Phys. Chem. Solids 8,119 (1959).
[13] J.R. Chelikowsky and M.L. Cohen, Phys. Rev. B 10, 5095 (1974).



ISBN 978-3-95450-126-7